Gordon H. Hall[1]
D. Moira Glerum[2,3]
Christopher J. Backhouse[1,3]

[1]Department of Electrical and Computer Engineering, University of Waterloo, ON, Canada
[2]Department of Biology, University of Waterloo, ON, Canada
[3]Waterloo Institute of Nanotechnology, University of Waterloo, ON, Canada

Received July 29, 2015
Revised September 3, 2015
Accepted September 4, 2015

Research Article

Light emitting diode, photodiode-based fluorescence detection system for DNA analysis with microchip electrophoresis

Electrophoretic separation of fluorescently end-labeled DNA after a PCR serves as a gold standard in genetic diagnostics. Because of their size and cost, instruments for this type of analysis have had limited market uptake, particularly for point-of-care applications. This might be changed through a higher level of system integration and lower instrument costs that can be realized through the use of LEDs for excitation and photodiodes for detection—if they provide sufficient sensitivity. Here, we demonstrate an optimized microchip electrophoresis instrument using polymeric fluidic chips with fluorescence detection of end-labeled DNA with a LOD of 0.15 nM of Alexa Fluor 532. This represents orders of magnitude improvement over previously reported instruments of this type. We demonstrate the system with an electrophoretic separation of two PCR products and their respective primers. We believe that this is the first LED-induced fluorescence microchip electrophoresis system with photodiode-based detection that could be used for standard applications of PCR and electrophoresis.

Keywords:
Genetic analysis / Light emitting diode induced fluorescence detection / Microchip electrophoresis / Microfluidics / Photodiode detection
DOI 10.1002/elps.201500355

Additional supporting information may be found in the online version of this article at the publisher's web-site

1 Introduction

Electrophoresis plays a central role in diagnostic technologies based on molecular biology; electrophoretic detection of fluorescently end-labeled DNA after PCR is a routine application. The miniaturization of electrophoresis to microchip electrophoresis or CE in conjunction with the promise of lab on chip is of particular interest for point of care applications, especially in conjunction with the potential for low cost rapid prototyped polymer chips [1]. Fluorescence detection is the standard method to visualize nucleic acid species analyzed by microchip electrophoresis [2], as it is readily applied to DNA with the use of end-labeled primers and is extremely sensitive. For a number of compelling reasons, primers with a fluorescent label at the 5'-end (referred to as end-labeled hereafter) have become the standard for most applications combining PCR and electrophoresis in the field of diagnostics [3]. End-labeled primers offer greater specificity (as only product(s) amplified by the appropriate primers are detected), absolute quantification of the fragment (as each fragment contains a single fluorophore), and higher electrophoretic precision (as all DNA fragments contain the same label and thus have similar shifts in mobility) [3]. Further, intercalators can non-specifically bind to channel walls and are typically classified as carcinogens, complicating their use.

The key challenge in lab on chip implementations of microchip electrophoresis is the LOD. A typical concentration of each primer in a PCR mixture is 100 nM (corresponding to 100 nM of fluorophore). For reasons of electrophoretic stability, typical diagnostic protocols require a 1 in 10 dilution of the PCR product with running buffer. Therefore, the LOD requirement for implementing these applications must be less than 10 nM and we have set 1 nM as a target. High sensitivity fluorescence detection for electrophoresis is typically done with instrumentation consisting of many large high performance components in a confocal or colinear

Correspondence: Dr. Christopher J. Backhouse, Department of Electrical and Computer Engineering, Waterloo Institute of Nanotechnology, University of Waterloo, 200 University Avenue West, Waterloo, Ontario N2L 3G1, Canada
E-mail: chrisb@uwaterloo.ca

Abbreviations: AF532, Alexa fluor 532; **APD**, avalanche photodiode; **BW**, buffer waste well; **GRIN**, gradient index; **PMT**, photomultiplier tube; **SW**, sample waste well

Colour Online: See the article online to view Fig. 2 in colour.

configuration with a laser, interference filter, dichroic beam splitter, photomultiplier tube (PMT), and lenses [4]. In colinear optical arrangements, the light source and detector use a common optical system to both focus excitation light and collect emission light [5] and as such requires a beamsplitter or dichroic filter to separate excitation and emission light. Often, an aligned pinhole is placed in the optical path to form a confocal optical setup with improved spatial resolution. While providing excellent LODs and low baselines, this leads to expensive instrumentation that does not lend itself to the integration needed for point of care applications. In a discussion on the commercialization of point of care diagnostics, Chin et al. noted the increasing demand for point of care nucleic acids testing [6] and they and others have identified cost as a central factor in determining the feasibility of point of care systems [6, 7]. We seek to address this by replacing costly and complex optical systems with LEDs for excitation (LED-induced fluorescence), absorption filters for optical filtering and photodiodes for light collection in an orthogonal configuration, much as described by Xiao et al. [5].

Compared to lasers and laser diodes, LEDs have the advantage of being substantially lower cost, requiring simpler drive electronics, having longer lifetimes, lower power consumption, higher signal stability, and lower temporal noise [8], all of which facilitate miniaturization. However, there are two central issues hindering LED usage for microchip electrophoresis. Firstly, LEDs have a broad output light spectrum that limits the efficiency of fluorophore excitation, due to poor spectral overlap, and can pass through the emission filter used, leading to high baselines. Typically an excitation filter is used to limit the baseline effect [8]. Secondly, LEDs have high étendue (i.e. poorly collimated light). This means that LED-based systems are less efficient in coupling the excitation light into the small optically probed volume required for good microchip electrophoresis detection. As a consequence, and as reviewed by Götz and Karst in 2007 [9], Xiao et al. in 2009 [5] and Macka et al. in 2014 [8], LED-induced fluorescence detection-based optics for microchip electrophoresis are rare.

The use of a photodiode has several advantages over PMTs or avalanche photodiodes (APDs). Most notably, photodiodes are many orders of magnitude less expensive. Further, photodiodes require substantially simpler detection electronics and do not need a high voltage bias, making them much easier to integrate. On the other hand, both PMTs and APDs have substantial gains (e.g. 10^5 for a PMT, versus no gain for a photodiode), and as a result of this, most LED-illuminated systems reported to date have relied on APDs (e.g. [10]) or PMTs (e.g. [11]).

Based on a literature search for all microchip demonstrations of LED-induced fluorescence with photodiode detection (e.g. not involving capillaries, PMTs or APDs), the only reports are those by Namasivayam et al. [12], the work by Webster et al. [13] and the work by Yang et al. [14]. In a recent review of advances in microchip electrophoresis by Castro and Manz [15], the work of Yang et al. (2011) has been cited as defining the state of the art for a LED and photodiode-based instrument for microchip electrophoresis, with a LOD of 100 nM fluorescein. Similarly, Macka et al. (2014) [8] also cite Yang et al. as representing the state of the art for LED-based microchip electrophoresis systems. This work is the best LOD reported to date for such systems. However, although this was an excellent demonstration of a good LOD with a low-cost design, it did not yet have sufficient performance for end-labeled electrophoretic PCR product analysis.

In the present work, we demonstrate a LED and photodiode-based microchip electrophoresis system that is capable of electrophoretic PCR product analysis. The system detection uses an improved optical system composed of blue LED illumination, plastic absorption filters, gradient index (GRIN) lenses, and a photodiode with an optimized transimpedance amplifier. The instrumentation is operated by a low cost microcontroller. The electrophoretic separations are done in agarose-filled rapid-prototyped plastic microchips with an LOD of 0.15 nM of end-labeled DNA (using Alexa fluor 532, AF532). We believe this to be the first photodiode and LED-based microchip electrophoresis system capable of implementing the "gold standard" for genetic diagnostic applications of electrophoretic analysis of end-labeled PCR products, with a LOD that is orders of magnitude better than previously reported for an LED and photodiode-based system.

2 Materials and methods

Genomic DNA was obtained with informed consent and purified with a commercial kit. Portions of exon 2 and 4 of the HFE gene were amplified with a Bio-Rad CFX q-PCR machine, resulting in products 234 and 436 bp long, respectively. Separations were performed in 2.5% agarose in a 0.5 x running buffer. Further detail can be found in the supporting information and in past work [16, 17].

2.1 Fluidic design and fabrication

The fluidic chips were micromilled using a computer numeric control milling machine. These fluidic chips were based on a simple cross design. The chip was operated by first applying an electric field across the injection channel, with high voltage applied to the sample waste well (SW) and ground applied to the sample well (S), drawing the sample across the intersection. The field was then switched to span the separation channel by applying a high voltage to the buffer waste well (BW) and ground to the buffer well (B). The chip is illustrated in Fig. 1. The distance from the intersection to the edge of S was 2 mm and the distance from the intersection to the detection point was 17 mm. Further detail can be found in the supporting information and has been previously reported [16, 17].

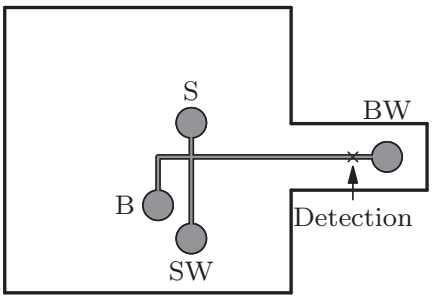

Figure 1. Schematic for the rapidly prototyped fluidic chip with a simple cross design. The injection distance was 2 mm (S to intersection) and the separation distance (from the intersection to the detection point) was 17 mm. The separation channel extends into a narrow 7 mm "neck" to improve the coupling efficiency of the LEDs at the detection point.

2.2 Microchip electrophoretic running protocol

The microchip electrophoresis running protocol was representative of that used in clinical diagnostic settings where a dilution of at least 1:10 of the PCR product is required (e.g. as in [3]). Two types of separations were carried out: LOD tests with fluorescently labeled PCR primer (no product), and DNA separations with the PCR products described above. The chip was first prepared by filling each well (S, SW, B, BW) with 10 μL 0.5 X running buffer. A preparation run was done by applying 58 V (61 V/cm) for 100 s across the injection channel and then applying 166 V (64 V/cm) for 480 s across the separation channel. The SW, B, and BW wells were then emptied and replaced with fresh 10 μL 0.5 X running buffer. The S well was emptied and filled with the sample. For the DNA separation test, the sample consisted of 1 μL each of both PCR products added to 8 μL of 0.5 X running buffer to make the 10 μL sample. For the LOD test, the sample consisted of 1 μL of a mock PCR mix (all the same reagents for a normal PCR but lacking polymerase enzyme and template) diluted with 9 μL of 0.5 X running buffer for a 10 μL sample resulting in a primer concentration of either 40, 4, or 0.4 nM. A separation run was done by applying 33 V (35 V/cm) for 80 s across the injection channel and then applying 166 V (64 V/cm) for 300 s across the separation channel. Data were collected with a nominal sampling rate of 500 Hz. Further detail can be found in the supporting information.

2.2.1 Data processing

The resulting electropherograms were processed with a standard data processing algorithm [17]. The algorithm first discounts all preseparation signal. Next any linear drift was removed with a single linear trend. It has been noted that LED output light decreases even at a stable current due to junction warming effects [8]. After the first 20 s of the LED being on, the LED warming drift was linear on the time scale of an electrophoretic separation. This drift was removed by first fitting a linear trend to the last 50 s of the separation and subtracting this trend from the whole signal. This also corrects for the baseline. A moving average taken over a 1 s window of acquisition time (500 points) was applied. This removed time domain noise not associated with the signal. The noise level of the signal was established by acquiring the standard deviation of the same portion of signal used for baseline estimation and removal. After data processing, the LOD was considered to be the concentration of fluorophore that gives a signal to noise ratio of 3.

2.2.2 Electronics

A microcontroller controlled the applications of high voltages generated using a DC-DC converter, high voltage relays, and spring-loaded contacts. The excitation light was controlled by the microcontroller via 2 current sources and the optical signal was read out through a two-stage transimpedance amplifier. This amplifier had a total effective gain of $5.1 \times 10^{10} \frac{V}{A}$ and was based on the two stage high gain amplifier designs from Graeme [18] for telecommunications applications. Those designs are optimized for high frequency regimes that are not suitable for electrophoretic applications where signals change with a very low frequency of ≈ 0.3 Hz. As such, we have modified this design for a low bandwidth, very low noise design. The first stage feedback resistance was 1 GΩ with a 20 pF added feedback capacitance giving a gain of $10^9 \frac{V}{A}$ and a bandwidth of 8 Hz. The added feedback capacitance increased the stability of the circuit and gave the system additional predictability as it was roughly two orders of magnitude higher than the stray capacitance [18]. The second stage of amplification was a noninverting amplifier circuit with a total gain of 51 $\frac{V}{V}$. The theoretical noise for the circuit was 0.17 $\frac{mV}{\sqrt{Hz}}$.

Both the circuit design and the instrumental assembly were focused on controlling noise sources. The entire system was shielded inside the aluminum enclosure to reduce electromagnetic pickup noise. This enclosure also cut leakage of ambient light into the system to negligible levels (necessary to ensure stable baselines). The first stage of amplification was routed through the air rather than through the board (a "flywire" design) to reduce surface leakage currents. We found that without this assembly technique the system was highly sensitive to ambient humidity and a stable baseline signal was not achievable. The measured noise for this circuit at full bandwidth was 4.6 mV with a nominal sampling rate of 500 Hz. Given that the noise was normally distributed and significantly larger than the quantization limit, our sensitivity was not limited by the analog digital converter quantization. The low noise electronics contributed strongly to the system performance. Further detail can be found in the supporting information.

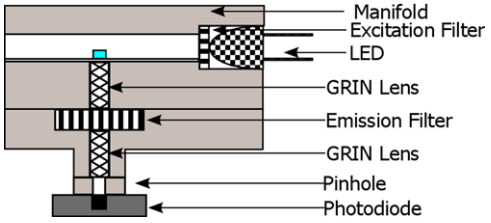

Figure 2. A diagram of the optics used. The sample is side illuminated with two LEDs (second LED not shown) that are filtered by a thin absorption filter. The emission light was collected by the GRIN relay and filtered. A pinhole was added to limit the optically probed volume and a photodiode was pressed against the bottom.

2.3 System design

2.3.1 Optics design

The optical system design is shown in Fig. 2. The design was based upon blue LED illumination, absorption filters, a photodiode, and GRIN lenses. Many works use interference filters for their high optical density (typically 5 or 6) with additional wavelength discrimination from the use of dichroic filters. However, these interference filters require up to 40 deposited layers with layer thickness controlled within 5% [4]. This makes them very expensive, both to purchase commercially as well as to be fabricated in integrated systems. Absorption filters, on the other hand, can be deposited in a single process with substantially relaxed constraints and negligible costs. Moreover, interference filter-based systems are dependent upon high degrees of collimation. Such collimation requires additional components and hinders integration. Hence, for future scalability and lower costs we have opted to use only plastic absorption filters.

The excitation pathway consisted of two blue LEDs (WP710A10QBC/G, Kingbright) shining through a thin (approx 100 μm) absorbing excitation filter (Sapphire Blue, Roscolux). Both LEDs were inserted into milled holes in the side of a holder that also served to heat-sink the LEDs. The chip allowed the LEDs to be held 3.5 mm from the channel and this proximity improved the efficiency of light injection. The emission pathway was based upon an optical relay arrangement in which two GRIN lenses (GRIN2306A, Thorlabs) image the photodiode active area (SFH2701, OSRAM Semiconductor) onto the bottom of the chip. The GRIN lens arrangement provides a high light collection efficiency due to their high numerical aperture and proximity to the channel [17]. In contrast to most other systems, the optically probed volume was limited horizontally by a 200 μm pinhole in the emission pathway rather than placing an aperture on the excitation path. This reduces the optical alignment tolerance between the excitation LED and the lens and simplified fabrication. Since low power LEDs were used, photobleaching of the sample was not apparent, unlike the situation commonly found with higher power LED or laser systems. In the vertical direction, the light collection efficiency drops substantially for distances greater than 100 μm away from the chip bottom [17]. The emission filter was a 3 mm thick piece of amber plastic (Acrylite 2C04, Evonik). We note the prior work of Floquet et al. [19] with absorbing acrylic-filters in absorbance-based optical measurements. The combination of the emission and excitation filters attenuated the total amount of excitation light (over all wavelengths) by 4.6 orders of magnitude, a value that is significantly less than when interference filters are used. As a result, the instrument had a substantial baseline (of $\approx$ 1V). However, since the LED illumination was very stable with only thermal drift effects present, the baseline variation was linear with time (after a warm-up period) and less than 1% of the baseline. This variation was easily removed in postprocessing.

3 Results

Upon automated testing over the course of a 48-h period without fluorescent materials present, the resulting noise level was determined to be 0.15 $\frac{mV}{\sqrt{Hz}}$, which is very close to the theoretical noise and thus corroborates our board design and assembly methods. This results in a LOD corresponding to 10 fW of fluorescent light. Further testing with separations of primers and product indicated additional noise was present (presumably from the amplification process), raising the noise by as much as another factor of 2.

Representative electropherograms for both the LOD determinations and DNA PCR product analysis are shown in Fig. 3. For the LOD test, the primer peak heights were 1.2, 8.1, and 103.5 mV for the PCR primer at concentrations of 0.4, 4, and 40 nM, respectively. For the two weakest peaks (i.e. for 0.4 and 4 nM, the two traces nearest the LOD), the LOD was 0.15 and 0.16 nM, respectively. (A comparable LOD can be estimated from the separations of the PCR products.)

For the DNA separation, the system detects both PCR products and resolves them completely. The Exon 4 product peak (furthest right) was 31 mV (signal to noise ratio = 207) in amplitude and the Exon 2 product was 62 mV (signal to noise ratio = 413) in amplitude, demonstrating that both products are detected by the instrument. We also detected a small primer-dimer peak at 127 s that was from the Exon 4 PCR and had a height of 12 mV (signal to noise ratio = 80). When optimizing a PCR, it is important to see these low level amplicons as they can complicate future analyses. This demonstrates the need to have a suitable (i.e. 1 nM or lower) LOD for this application. The separation of the two PCR products also allows for the estimation [3] of the resolution with Eq. (1):

$$Res = (s_2 - s_1) \times \frac{w_1 + w_2}{2 \times (t_2 - t_1)}, \quad (1)$$

where s_x is the size of product x in bp, t_x is the arrival time of product x and w_x is the full width at half max (FWHM) of product x. The resolution in our system was calculated to be 49 bp . This value is comparable to the 50 bp resolution obtained on similar fluidics in the past [16] using a laser and PMT-

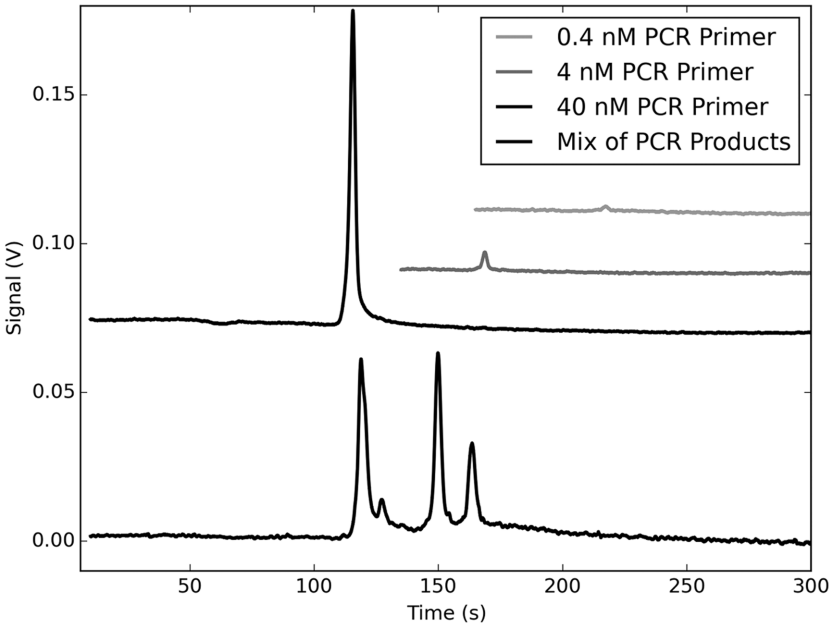

Figure 3. Representative electropherograms from the system. The bottom trace is a separation of two PCR products from primers and, as a series dilution, the higher traces are separation of the unamplified PCR primers at concentrations of 0.4, 4, and 40 nM with signals of 1.2, 8.1, and 103.5 mV, respectively. The corresponding signal to noise levels (with noise standard deviations calculated as described above) were 8, 74, and 345, respectively. For ease of display, the 40 nM primer trace was offset vertically by 80 mV with the traces from lower concentrations successively offset vertically by 20 mV each, and horizontally by 60 and 90 s. In the bottom trace, the peak identities for the product mixture (from left to right) are primer, primer-dimer from the exon 4 reaction, HFE exon 2 PCR product (234 bp), and HFE exon 4 product (436 bp).

based commercial confocal optics system. This may indicate that the resolution here is limited by the electrophoretic separation itself. Although we could achieve higher resolutions with longer channels and other sieving matrices, the agarose gel is convenient to work with.

4 Discussion

The LOD of 0.15 nM of AF532 meets the requirement for analysis of end-labeled PCR product, detecting PCR products with signal to noise ratios that are over 100. In order to compare the LOD of this system to previous work, we scale for the variations in materials parameters, since some fluorophores emit or absorb more strongly than others. The scaling factor used here is the product of the maximum extinction coefficient of the fluorophore (how well the fluorophore absorbs excitation light) and the fluorophore quantum efficiency (how well the fluorophore converts absorbed excitation light to emission light). The parameters for the three most relevant fluorophores are shown in Table 1. Table 2 reflects all known reports in the literature for LED + photodiode-based microchip electrophoresis instruments whether as found by us or as reviewed by either Castro and Manz [15], Macka et al. [8], or Xiao et al. [5]. The primary comparison is that of Yang et al., but given the lack of other reports we also compare our results to intercalator-based work. The scaling factor is normalised to the value for AF532, a fluorophore that is representative of those used in end-labeled analyses and the one that was used in the present work. The scaled LODs are the estimates of the values that would have been reported if all research had used the same fluorophore (AF532) as an end-label.

Table 1. Fluorophore scaling factors used for LOD comparisons. The scaling factor is the product of the extinction coefficient and the quantum yield, normalized to Alexa Fluor 532, a representative end-label for DNA applications. The scaling factor allows for the comparison of different systems as shown in Table 2. In the basic borate buffer used in Yang et al., the fluorescein dianion dominates the observed fluorescence [26]. As such, we have used the properties of the dianion for the scaling factor

Fluorophore	Quantum yield	Extinction ϵ coeff. ($M^{-1}cm^{-1}$)	Scaling factor
Alexa Fluor 532	0.61 [22]	81 000 [23]	1
Fluorescein	0.93 [24]	76 900 [24]	1.45
Yoyo-1	0.52 [25]	98 900 [25]	1.04

We have carried out this development with end-labeled primers because there are a number of significant disadvantages associated with the use of intercalators, particularly as it applies to molecular diagnostics applications. The intercalation of a fluorescent dye into DNA causes changes in the conformation of the DNA molecule, resulting in alterations during electrophoresis. Perhaps more importantly, the intercalation reduces the net charge of the DNA molecule and thereby also reduces its mobility. As discussed by Barron and Blanch [20], this altered migration could render futile any attempts to quantify differences in DNA fragment mobilities between samples. For example, an assay designed to detect slight differences in the size of PCR fragments, such as those associated with small deletions or insertions, would not be reliable given the effects of the intercalator on DNA mobility. This problem can be magnified by the variable number of fluorophores that intercalate into the DNA molecules, depending on the ratio of DNA/intercalator. This characteristic

Table 2. Comparison of the LOD for this system with other LED + photodiode detector-based microchip electrophoresis instruments. The effective LOD is calculated by removing stacking effects, correcting for the fluorophore as described for Table 1 and accounting for the multiple-labeling of intercalators

Work	Cited limit of detection (nM)	Fluorophore	Comments	Effective AF532 LOD (nM)
This work	0.15	AF532	–	0.15
Hall et al. [17]	2	AF532	Stacking effects removed, dilution accounted for	1
Yang et al. [14]	100	Sodium fluorescein	–	145
Namasivayam et al. [12]	0.9 $\frac{ng}{\mu L}$ DNA	Yoyo-1	Intercalator	341

also hinders accurate quantification of the DNA. Intercalators, especially the dimeric dyes such as ethidium bromide, are also notoriously prone to adsorption to the channel walls, causing significant distortions to the peaks. Other drawbacks associated with intercalators are the presence of a single color, preventing multiplexing of the assay, and the fact that intercalators such as ethidium bromide are classified as carcinogens, precluding their use by untrained operators. For these reasons, the use of intercalating dyes is not standard for diagnostic applications, although they do have the advantage of producing a stronger optical signal, as an intercalating fluorophore can bind to 1 in 4 [21] base pairs. For comparative purposes, we include the most relevant intercalator work we are aware of, the (YOYO-1) work of Namasivayam et al. [12]. The work of Namasivayam et al. does not cite the ratio of fluorophores to number of base pairs. However, we use the ratio they previously reported [13] (of 1 fluorophore per 5 base pairs of DNA) to estimate the AF532-equivalent LOD for their system.

Another issue that needs to be taken into account is that of sample stacking. Sample stacking makes use of a variation in channel conductivity (transient in nature) to increase the concentration of sample injected. Since sample stacking is a procedural phenomenon rather than an instrumental one, and because sample stacking is highly time-dependent (and hence a source of variability) we have removed the LOD enhancement due to sample stacking from our comparative figures. To compare with our previous work [17], we remove the effect of sample stacking and we now calculate the LOD in the same manner as used for all the other reports given here, i.e. the LOD in terms of the concentration in the sample well itself.

In comparison to the state of the art for LED and photodiode-based microchip electrophoresis instruments, i.e. the report by Yang et al., the present system improves on that LOD by more than two orders of magnitude (from 145 to 0.15 nM). This improvement is crucially important as it brings the LOD to well below the threshold required for end-labeled PCR product electrophoretic analysis. The system was tested both with PCR primers of known concentration, for LOD assessment, as well as with a separation of two PCR products from their primers.

Namasivayam et al. [12] and the group's previous work by Webster et al. [13] are excellent examples of miniaturized microchip electrophoresis systems with tightly integrated combinations of channel, photodiode, and LED. However, these devices did not reach LOD levels required for end-labeled DNA use. Further, these were based on the use of 40 layer (the former) or 20 layer (the latter) interference filters that would be highly problematic to integrate into a commercial CMOS fabrication technology.

We note related work in academia. In particular we note the APD-based work of Chabinyc et al. [10] who demonstrated an integration of a blue LED, optical fiber, and polymer absorbing filters with an APD in PDMS chips. That work achieved an effective LOD of 5.4 nM AF532, a LOD that is sufficient for end-labeled diagnostic use (though it is an order of magnitude higher than that of the present work and was based on an APD). We also note some promising advances in colinear optical detectors for capillaries. Prikryl and Foret recently demonstrated the use of an LED, interference filters and photodiode (with integrated gain) to achieve an impressive 92 pM fluorescein (0.13 nM AF532) LOD [27]. As another example, Wu et al. [28] demonstrated a system with an APD that achieved a LOD of 0.2 nM fluorescein (0.29 nM AF532). The LODs for these systems are similar to the system presented here, however their use of colinear optics (and in the case of Wu et al., use of an APD) and substantially higher component costs precludes further integration.

As noted by Eijkel, to date, commercial point of care applications of microchip electrophoresis have been limited by sensitivity [29]. Commercial microchip electrophoresis systems in the more general field of microchip electrophoresis (i.e. not restricted to point of care microchip electrophoresis) typically use colinear or confocal optics and hence are difficult to compare to this work (or to use in a point of care setting). The Hitachi SV 1100 is a microchip electrophoresis optical module based upon an LED, confocal optics and an APD, with a LOD cited to be μM to sub μM [9]. Most other systems are based on intercalating dyes. Both of the laser-based systems, the Bio-Rad Experion system and Perkin Elmer LabChip (formerly Caliper), have cited LODs of 0.1 ng/μL [30], [31], a value that corresponds to 1.6 nM fluorophores (conservatively assuming an intercalation ratio of 1 fluorophore: 100 base pairs,

a very light labeling). (If instead we assume that they used the same intercalation ratio as used above, i.e. 1:5 as for Webster et al. [13] and Namasivayam et al. [12], we would have obtained a LOD of about 30 nM.) Hence, the present work has attained similar or significantly better LODs without the use of lasers or confocal optics.

In previous work, we had demonstrated a similar system that was largely based upon a single CMOS microelectronic chip and showed how optical relay systems, such as this work, scale to a miniaturized instrument where channels and electronics are fabricated monolithically using Teledyne-DALSAâs combined CMOS/microfluidic technology [17]. The LOD of that system was approximately 1 nM, only one order of magnitude less than a typical PCR product. To further enhance the LOD, in that work we utilized sample stacking techniques that gained another factor of 5 in LOD (although that enhancement was transient in nature and thereby complicated protocol optimization due to varying mobilities in the injection and separation channels). That system was built upon an experimental CMOS chip that ultimately proved to be short lived, likely due to a combination of electrostatic discharge and power on transients; we realized after the fact that we had not considered all possibilities for the system startup conditions. This design has since been improved. While further developments are underway, we expect to continue to optimize our designs using discrete components as in this work. This design uses a similar GRIN lens-based optical relay such that it, too, scales to a single chip system where the lenses will no longer be required. Currently, the cost of the components within the present optics is less than $100, where more than 90% of this cost is from the two lenses. Therefore, we expect our future optical component cost after single chip integration to be under $10, enabling point of care applications.

In conclusion, we demonstrate a LED-photodiode-based microchip electrophoresis instrument with a LOD of 0.15 nM, orders of magnitude better than previously reported, and one that is capable of end-labeled PCR product analysis. To echo the words of Forster et al. [32], the remarkable versatility of microchip electrophoresis is such that one might expect microchip electrophoresis to enable important applications. It is our hope that the present demonstration will lead to the development of important commercial applications of electrophoresis in point of care settings.

We would like to acknowledge Chanele Polenz and Madeline H. Couse for their contributions to the molecular biology and Victor Shadbolt and Hirad Raisi for their contributions to the infrastructure used in this demonstration. We would also like to acknowledge that the manuscript benefited from valuable suggestions from our reviewers. The work itself was funded through a grant from the Natural Sciences and Engineering Research Council of Canada (NSERC), with the support of Teledyne-DALSA.

The authors declare that they have no conflict of interest.

5 References

[1] Becker, H., *Talanta* 2002, *56*, 267–287. [Online]. Available at: http://linkinghub.elsevier.com/retrieve/pii/S003991400100594X.

[2] Hernandez, L., Escalona, J., *J. Chromatography* 1991, *559*, 183–196. [Online]. Available at: http://www.sciencedirect.com/science/article/pii/002196739180069S.

[3] Life Technologies, "DNA fragment analysis by capillary electrophoresis," 2014. [Online]. Available at: http://tools.thermofisher.com/content/sfs/manuals/4474504.pdf.

[4] Dandin, M., Abshire, P., Smela, E., *Lab Chip* 2007, *7*, 955. [Online]. Available at: http://www.ncbi.nlm.nih.gov/pubmed/17653336 http://xlink.rsc.org/?DOI=b704008c.

[5] Xiao, D., Yan, L., Yuan, H., Zhao, S., Yang, X., Choi, M. M. F., *Electrophoresis* 2009, *30*, 189–202. [Online]. Available at: http://doi.wiley.com/10.1002/elps.200800415.

[6] Chin, C. D., Linder, V., Sia, S. K., *Lab Chip* 2012, *12*, 2118–2134. [Online]. Available at: http://www.ncbi.nlm.nih.gov/pubmed/22344520.

[7] Laxminarayan, R., Mills, A. J., Breman, J. G., Measham, A. R., Alleyne, G., Claeson, M., Jha, P., Musgrove, P., Chow, J., Shahid-Salles, S., Jamison, D. T., *Lancet* 2006, *367*, 1193–1208. [Online]. Available at: http://linkinghub.elsevier.com/retrieve/pii/S0140673606684407.

[8] Macka, M., Piasecki, T., Dasgupta, P. K., *Ann. Rev. Anal. Chem.* 2014, *7*, 183–207. [Online]. Available at: http://www.annualreviews.org/doi/abs/10.1146/annurev-anchem-071213-020059.

[9] Götz, S., Karst, U., *Anal. Bioanal. Chem.* 2006, *387*, 183–192. [Online]. Available at: http://link.springer.com/10.1007/s00216-006-0820-8.

[10] Chabinyc, M. L., Chiu, D. T., McDonald, J. C., Stroock, A. D., Christian, J. F., Karger, A. M., Whitesides, G. M., *Anal. Chem.* 2001, *73*, 4491–4498.

[11] Miyaki, K., Guo, Y., Shimosaka, T., Nakagama, T., Nakajima, H., Uchiyama, K., *Anal. Bioanal. Chem.* 2005, *382*, 810–816. [Online]. Available at: http://link.springer.['com/10.1007/s00216-004-3015-1.

[12] Namasivayam, V., Lin, R., Johnson, B., Brahmasandra, S., Razzacki, Z., Burke, D. T., Burns, M. A., *Journal of Micromechanics and Microengineering* 2003, *14*, 81–90. [Online]. Available at: http://stacks.iop.org/0960-1317/14/i=1/a=311?key=crossref.2eb189169fd75905fb4e167871a17e36.

[13] Webster, J. R., Burns, M. A., Burke, D. T., Mastrangelo, C. H., *Anal. Chem.* 2001, *73*, 1622–1626. [Online]. Available at: http://pubs.acs.org/doi/abs/10.1021/ac0004512.

[14] Yang, F., Li, X.-C., Zhang, W., Pan, J.-B., Chen, Z.-G., *Talanta* 2011, *84*, 1099–1106. [Online]. Available at: http://dx.doi.org/10.1016/j.talanta.2011.03.020 http://linkinghub.elsevier.com/retrieve/pii/S0039914011002256.

[15] Castro, E. R., Manz, A., *J. Chromatography A* 2015, *1382*, 66–85. [Online]. Available at: http://dx.doi.org/10.1016/j.chroma.2014.11.034 http://linkinghub.elsevier.com/retrieve/pii/S0021967314017920.

[16] Ma, T., Northrup, V., Fung, A. O., Glerum, D. M., Backhouse, C. J., in: Kieffer, J.-C. (Ed.), *Proc. SPIE*, Ottawa, vol. 8412, 2012, 84120B. [Online]. Available at: http://proceedings.spiedigitallibrary.org/proceeding.aspx?articleid=1387270 http://proceedings.spiedigitallibrary.org/proceeding.aspx?doi=10.1117/12.2001470.

[17] Hall, G. H., Sloan, D. L., Ma, T., Couse, M. H., Martel, S., Elliott, D. G., Glerum, D. M., Backhouse, C. J., *J. Chromatography A* 2014, *1349*, 122–128. [Online]. Available at: http://www.ncbi.nlm.nih.gov/pubmed/24856905http://linkinghub.elsevier.com/retrieve/pii/S0021967314007249.

[18] Graeme, J., *Photodiode Amplifiers*, McGraw-Hill, New York 1996.

[19] Floquet, C. F., Sieben, V. J., Milani, A., Joly, E. P., Ogilvie, I. R., Morgan, H., Mowlem, M. C., *Talanta* 2011, *84*, 235–239. [Online]. Available at: www.ncbi.nlm.nih.gov/pubmed/21315925http://linkinghub.elsevier.com/retrieve/pii/S0039914010010167.

[20] Barron, A. E., Blanch, H. W., *Sep. Purif. Rev.* 1995, *24*, 1–118.

[21] Waring, M., *J. Mol. Biol.* 1965, *13*, 269–282. [Online]. Available at: http://dx.doi.org/10.1016/S0022-2836(65)80096-1http://linkinghub.elsevier.com/retrieve/pii/S0022283665800961.

[22] Life Technologies, "Fluorescence quantum yields (QY) and lifetimes (τ) for Alexa Fluor dyesâTable 1.5." [Online]. Available at: https://www.lifetechnologies.com/ca/en/home/references/molecular-probes-the-handbook/tables/fluorescence-quantum-yields-and-lifetimes-for-alexa-fluor-dyes.html.

[23] Life Technologies,–, "The Alexa Fluor Dye SeriesâNote 1.1," [Online]. Available: https://www.lifetechnologies.com/ca/en/home/references/molecular-probes-the-handbook/technical-notes-and-product-highlights/the-alexa-fluor-dye-series.html.

[24] Sjöback, R., Nygren, J., Kubista, M., *Spectrochim. Acta Part A* 1995, *51*, L7–L21. [Online]. Available at: http://linkinghub.elsevier.com/retrieve/pii/058485399501421P.

[25] Benvin, A. L., Creeger, Y., Fisher, G. W., Ballou, B., Waggoner, A. S., Armitage, B. A. *J. Am. Chem. Soc.* 2007, *129*, 2025–2034.

[26] Martin, M. M., Lindqvist, L., *J. Luminescence* 1975, *10*, 381–390. [Online]. Available at: http://linkinghub.elsevier.com/retrieve/pii/0022231375900034.

[27] Prikryl, J., Foret, F., *Anal. Chem.* 2014, *86*, 11 951–11 956. [Online]. Available at: http://pubs.acs.org/doi/abs/10.1021/ac503678n.

[28] Wu, J., Liu, X., Wang, L., Dong, L., Pu, Q., *Analyst* 2012, *137*, 519.

[29] Eijkel, J., *Bioanalysis* 2015, *7*, 1385–1387. [Online]. Available at: http://www.future-science.com/doi/10.4155/bio.15.64.

[30] Bio-Rad Laboratories Inc., "Experion Automated Electrophoresis System." [Online]. Available at: http://www.bio-rad.com./webroot/web/pdf/lsr/literature/Bulletin_3140.pdf.

[31] Perkin Elmer, "LabChip Microfluidics Product Note," 2015. [Online]. Available at: http://www.perkinelmer.ca/en-ca/CMSResources/Images/44-161587PRD_LabChip-GX-Touch-DNA-Assays.pdf.

[32] Forster, R. E., Hert, D. G., Chiesl, T. N., Fredlake, C. P., Barron, A. E., *Electrophoresis* 2009, *30*, 2014–2024. [Online]. Available at: http://doi.wiley.com/10.1002/elps.200900264.

